Peremennye Zvezdy (*Variable Stars*) **42**, No. 11, 2022

Received 5 November; accepted 23 November.

DOI: 10.24412/2221-0474-2022-42-87-105

Long-term Brightness and Color Variations of the Young Variable Star V645 Cyg

S. Yu. Gorda, A. P. Bisyarina, A. M. Sobolev, S. Yu. Parfenov

Kourovka Astronomical Observatory, Ural Federal University, Mira str. 19, Yekaterinburg, 620002 Russia

We presents the results of our 13-year (2009–2022) photometric study of the young variable star V645 Cyg, which is a Herbig Ae/Be object located in a region of active star formation. Observations were carried out in the optical part of the spectrum, in VRI filters. During the observation time interval, we found, along with short-term small-amplitude chaotic brightness changes of V645 Cyg, we found a monotonous increase in the total brightness of the system in the V band by $\sim 1^{\rm m}$; in R, by $\sim 1\overset{\rm m}{.}4$; and in I, by $\sim 2^{\rm m}$, as well as an increase in the reddening of the system: its $V-R$ color index increased by $\sim 0\overset{\rm m}{.}3$, and $R-I$, by $\sim 0\overset{\rm m}{.}6$. Optical brightness variations in the time interval JD 2450000–2456500 are closely followed by variations of the CH_3OH maser flux at 6.7 GHz reported in the literature. Absence of strong variations on the time scale of hours suggests that non-stationarity effects in the maser radiation are not significant. The monotonous changes in the brightness and color of V645 Cyg are interpreted as a decrease in the optical depth of the gas-dust cocoon towards the star and corresponding increase in the visibility of regions of the star and its immediate vicinity.

Variability of V645 Cyg was discovered by Hoffmeister et al. (1951). Cohen (1977) found that the position of V645 Cyg coincided, within $5''$, with a reflection nebula and found three condensations (N0, N1 and N2 in his notation) from spectrophotometry and spectropolarimetry. He came to the conclusion that the star itself, whose radiation is reflected by the condensations, is a young star of the spectral type O and, most likely, is situated between the starlike knot N0 and the knot N1, partially being in a gas-dust cocoon. Further studies of the object V645 Cyg, mainly in the infrared (IR) and radio ranges (Humphreys et al., 1980; Lada et al., 1981; Morris et al., 1982; Torrelles et al., 1983; Goodrich, 1986), revealed bipolar gas outflows, suggestive of the presence of a molecular protoplanetary disk observed in the IR range and in the maser lines of CH_3OH and H_2O (Valtts et al., 2002). The maser emission in OH transitions was also detected (Morris et al., 1982).

More recent mid-infrared studies of V645 Cyg have shown that N0 is a point source, i.e. a young star, and the nebular component N1, located five arc seconds northwest of N0, is a diffuse nebula, especially since the N0 component is 200 times brighter than N1 (Clarke et al., 2006). Thus, it became clear that N0 was the star V645 Cyg itself, and not just a knot of a reflection nebula such as N1, as it had been previously thought. Various observations show that V645 Cyg is a very complex and interesting object to study, containing a young massive star.

Despite the general opinion that V645 Cyg is a young stellar object, there is still no consensus on its physical parameters. Some authors prefer the classification of an O-type star (e.g., Testi et al., 1998), while others consider it an A-type supergiant (e.g., Bowey et al., 2003). The distance to the object was also ambiguous, ranging from 3 to 6 kiloparsecs (Clarke et al., 2006). The first measurement of trigonometric parallax from H_2O maser observations corresponds to a distance of 5.28 kpc (Honma et al., 2007),

but later measurements indicate a smaller value of 4.054–4.15 kpc (Asaki et al., 2014; Quiroga-Nuñez et al., 2019).

According to one of the recent studies (Miroshnichenko et al., 2009), V645 Cyg is a young massive B-type main sequence star that has already passed the stage of protostellar accretion and is being released from its gas-dust cocoon. Such young stellar objects are rare because they are quite massive and evolve rapidly. They are usually deeply embedded in the dust shell and their radiation manifests itself only in the IR range (Zinnecker et al., 2007). V645 Cyg is one of the few objects of this class visible in optics. One of the reasons for this is the orientation of the circumstellar disk plane, which practically coincides with the sky plane (Valtts et al., 2002; Miroshnichenko et al., 2009). Optical and IR images of the star contain two bright regions, which are interpreted as radiation from the disk and envelope (Cohen, 1977; Goodrich, 1986).

The angular size of the IR image increases with wavelength in the near- and mid-IR and decreases towards the millimeter range (Quiroga-Nuñez et al., 2019; Miroshnichenko et al., 1999). Based on medium-resolution spectroscopy data, Hamann and Persson (1989) suggested that these bright regions could represent reflected light from the disk and bipolar outflows.

The study of the V645 Cyg brightness changes was carried out mainly in the IR range. There are only two series of observations in the optical range, these are the very first photographic observations of Hoffmeister et al. (1951) in the 1950s and photoelectric observations by Shevchenko et al. (1993) in 1985–2000. Miroshnichenko et al. (2019), based on the analysis of the photometric data from Shevchenko et al. (1993) obtained in the $UBVR$ filters at the Maidanak observatory, indicate the possible presence of an 8-year variability period of the star's optical brightness with an average amplitude in the V band $\sim 0\overset{\mathrm{m}}{.}6$ and a decrease of the IR brightness at time scales of the order of 20 years. Interpreting the speckle interferometry data, Miroshnichenko et al. (2009) subdivided the K-band image of the star into two components. The bright, small ring component (radius $r \sim 25$ a.u.) is probably the emission from the disk near the sublimation front. The second component ($r \sim 250$ a.u.) may correspond to the emission of the circumstellar shell's inner part, but the authors emphasize that one cannot exclude, for example, this emission being light reflected off the boundary of the cavity formed by bipolar outflows.

Since photometric observations of V645 Cyg in the optical range were very rare, and the latest of them date back to 2000, new observations are extremely useful, at least in terms of confirming the periodic brightness variation discovered by Miroshnichenko et al. (2009).

Table 1: **Designations and coordinates of the observed stars**

Name	star	$\alpha(2000)$	$\delta(2000)$	m_V
V645 Cyg	variable	$21^{\mathrm{h}}39^{\mathrm{m}}58\overset{\mathrm{s}}{.}3$	$+50°14'21''$	$13\overset{\mathrm{m}}{.}50$
UCAC3 281-203713	comparison	$21^{\mathrm{h}}39^{\mathrm{m}}52\overset{\mathrm{s}}{.}5$	$+50°15'52''$	$12\overset{\mathrm{m}}{.}60$
UCAC3 281-203646	check	$21^{\mathrm{h}}39^{\mathrm{m}}47\overset{\mathrm{s}}{.}6$	$+50°17'01''$	$12\overset{\mathrm{m}}{.}22$

Our optical photometric observations of V645 Cyg were carried out on 111 nights from May, 2009 to March, 2018 using the AZT-3 reflector ($D = 0.45$ m, $F_{\mathrm{Newton}} = 2.0$ m) and from December, 2018 to April, 2022, using the AstroSib-500RC Ritchey–Chretién telescope ($D = 0.5$ m, $F = 4.0$ m) of the Kourovka Astronomical Observatory (Ural Federal University). Observations were carried out in the VRI filters, reproducing a system close to the Johnson–Cousins system when observing with Apogee Alta U6 CCD

cameras and a Kodak KAF-1001E chip (1024 × 1024, 24 μm) and, since 2015, with a PL A230 camera of the company FLI and an E2V 230-42 CCD chip (2048 × 2048, 15 μm). Two stars were chosen as a comparison star and a check star in the immediate vicinity of the variable, the data on them are given in Table 1. The coordinates in the Table are based on the Gaia-DR3 catalog.

After photometric processing, which included subtracting dark frames, dividing into flat-field frames, and determining the brightness of stars by aperture photometry, we obtained 111 night-averaged values of the brightness differences between V645 Cyg and the comparison star in the V filter, 96 values in the R filter, and 58 values in the I filter. The aperture size was chosen to cover the whole radiation associated to V645 Cyg in the given filter (including components N0 and N1). The light curves for V645 Cyg obtained over the 13-year observation period are shown in Fig. 1, Fig. 2 and Fig. 3. Data are given in Tables 2–6.

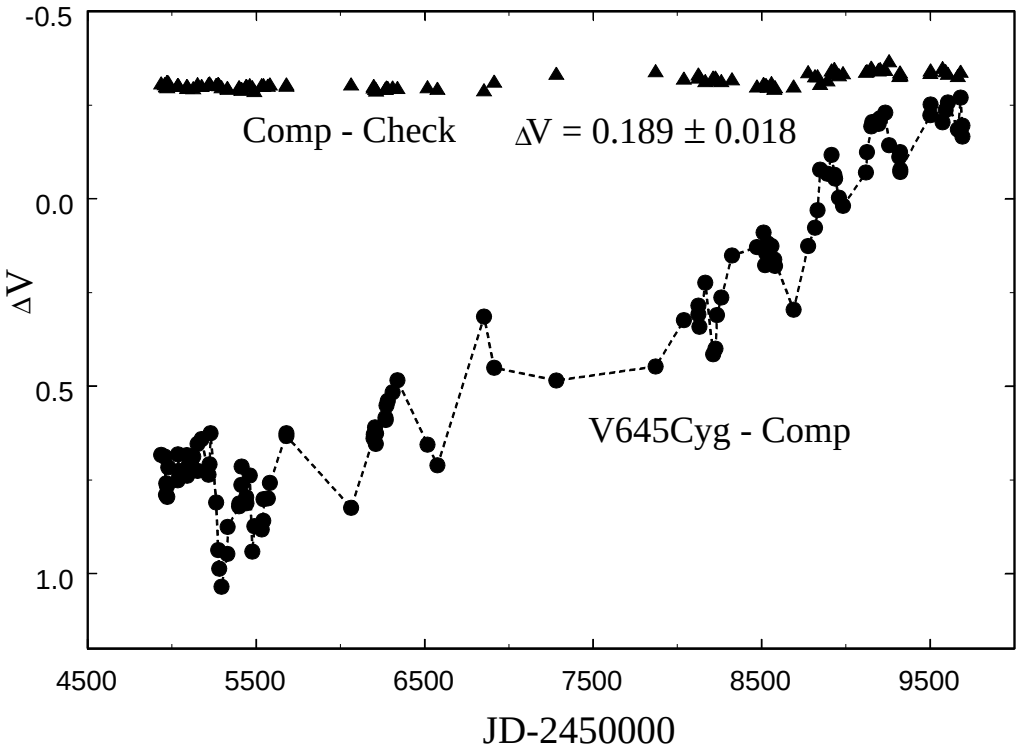

Figure 1. The V645 Cyg light curve in the V filter (circles) and the differences in the brightness of the comparison and check stars (triangles). In the upper part of figure, the values of difference between the magnitudes of the comparison star and the check star, averaged over the entire observation period, and the root mean square error are given.

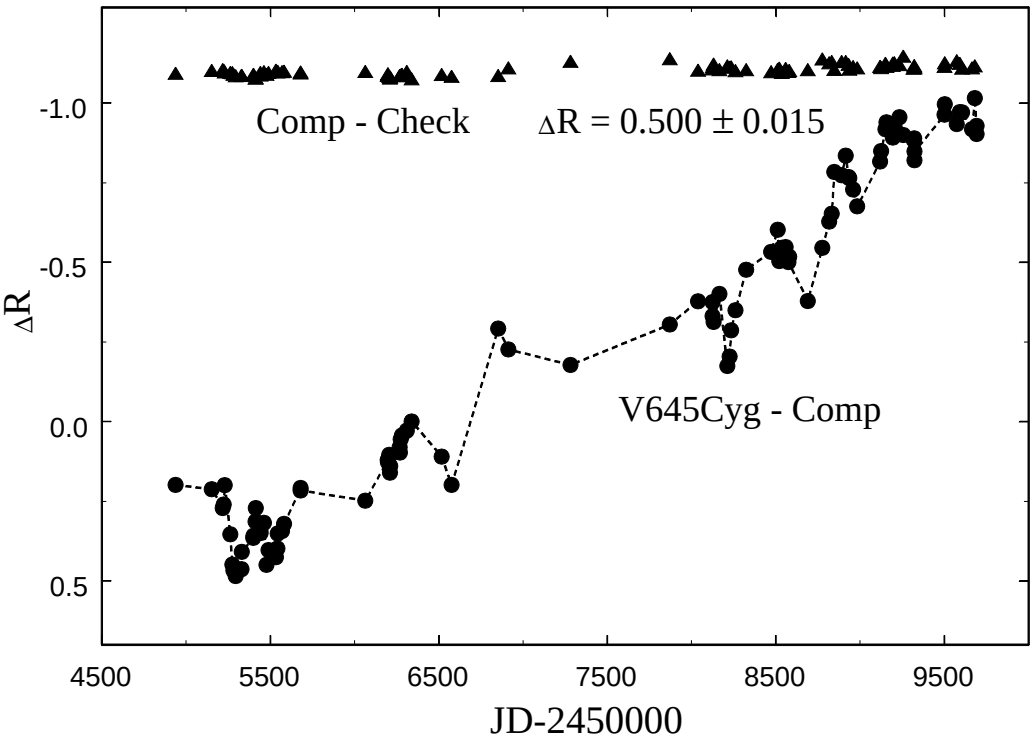

Figure 2. The V645 Cyg light curve in the R filter. Designations are the same as in Fig.1.

As can be seen, a systematic star brightness increase was observed throughout 13 years of our observations along with brightness changes of V645 Cyg with amplitudes from several hundredths to tenths of a magnitude over time intervals from a day to several months. At the same time, the brightness of the comparison star, as can be seen in Fig. 1, Fig. 2 and Fig. 3, remained practically unchanged within the limits of observational errors. Also, the average brightness of V645 Cyg in the V band has increased over 13 years by $\sim 1.0^m$, in the R band by $\sim 1.4^m$, and in the I band by $\sim 2.0^m$.

It can be noted that, along with an increase in brightness, the reddening of the star is also observed, which is clearly seen in the plots of $V-R$ and $R-I$ color indices change over time, shown in Fig. 4 and Fig. 5, respectively. Over the entire observation period, the color index $V-R$ increased by $\sim 0.3^m$, and $R-I$ by $\sim 0.6^m$. A change in the optical brightness within $\sim 0.5^m$ was also observed earlier in the data obtained by Shevchenko et al. (1993) (see Miroshnichenko et al., 2009). However, the same paper notes that the color indices $V-R$, as well as $B-V$ and $U-B$, remained stable within 0.1^m, which is significantly less than the amplitude of the changes in the data obtained from observations at the Kourovka Observatory.

We also did not find any periodicity in the brightness variations of V645 Cyg, especially with a period of 8 years, which was found by Miroshnichenko et al. (2009) in the observations of Shevchenko et al. (1993). Apparently, the periodic change in the optical brightness of this star occurs only during a certain time interval and is not a constant

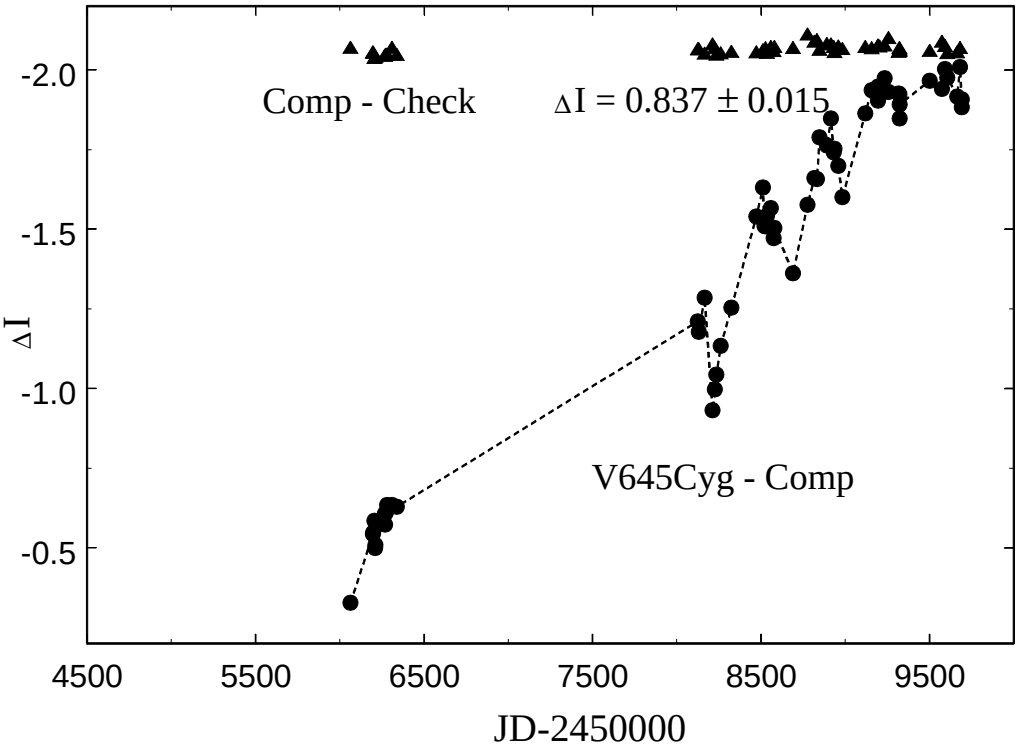

Figure 3. The V645 Cyg light curve in the I filter. Designations are the same as in Fig.1.

phenomenon.

It is important to note that optical brightness variations in the time interval $JD - 2450000 < 6500$ are closely followed by the variations of CH_3OH maser flux at 6.7 GHz presented by Szymczak et al. (2018). The increase in optical brightness corresponds to the increase of maser brightness and vice versa. Szymczak et al. (2018) found that the maser flux variations were quasi-periodic with a period of 195 days. Based on the observed correspondence between the maser and optical brightness variability, it can be assumed that the optical brightness variations at time scales of the order of 100 days are also quasi-periodic. As shown by Kojima et al. (2018) for the object G33.641-0.228, CH_3OH maser bursts can be observed on time scales of the order of several hours. Taking into account that the propagation speed of radiation, which affects the pumping of masers, can be significantly lower than the speed of light (Burns et al., 2020) and that the relaxation time of the CH_3OH level populations can be of hours, the interpretation of such maser variability that fast may require to take into account the non-stationary radiation transfer and excitation in the CH_3OH transitions. Our data shows that changes in the optical brightness during a night are mostly monotonic (see also Sobolev et al., 2013). Thus, based on our data in the optical range, we can assume that there are no strong sudden changes of CH_3OH masers in V645 Cyg on time scales of the order of several hours.

The data obtained by us during thirteen years of photometric observations of the young irregular variable star V645 Cyg are, in essence, the second monitoring series obtained

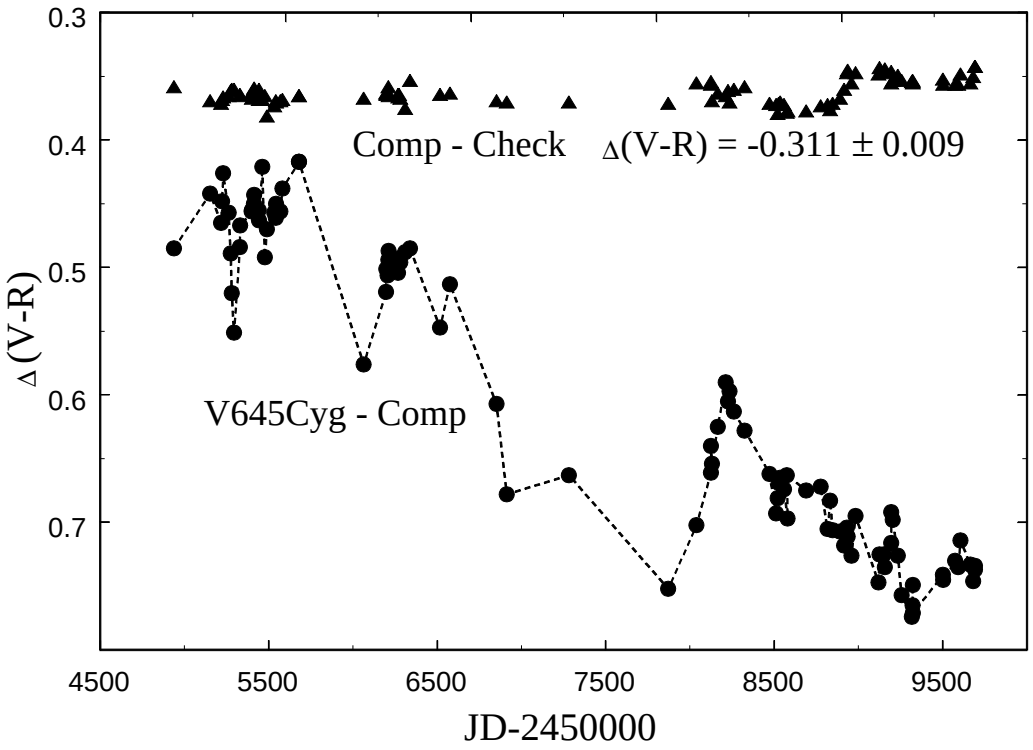

Figure 4. The time dependence of the differences between the $V - R$ color indices of V645 Cyg and the comparison star. Designations are the same as in Fig.1.

in the optical range in the process of studying this star using modern detectors. In this period of observations, in contrast to the results of the earlier optical monitoring of V645 Cyg (see Shevchenko et al., 1993), along with changes in brightness, a significant change in the color indices towards increasing reddening of the star was also observed.

Based on the results of this series of observations, as well as on data obtained at the same time in the IR range (Shenavrin et al., 2011), a number of conclusions can be drawn about the reasons for such changes in the brightness and color of V645 Cyg. These changes can be due to a change in the angle of inclination of the disk plane due to precessional rotation, during which hot structures in the inner region of the disk become more visible to the observer. Another possible scenario explaining the variability in optics and IR can be similar to that presented by Parfenov & Sobolev (2014). In this scenario, a spiral density wave in the inner disk region formed due to multiplicity of the system can propagate up to the radius of the sublimation front. There is a layer of hot gas at the end of the spiral wave near the surface of the star. During rotation, this heated layer is on the line of sight, the hot substance can approach the gas and dust inhomogeneities on the inner boundary of the disk and heat them up. This scenario, however, assumes that the variability of the CH_3OH maser flux at 6.7 GHz can be different for different components of the maser spectrum, which are formed in different regions in the vicinity of the star. The observed variability of the maser emission, which is in good agreement

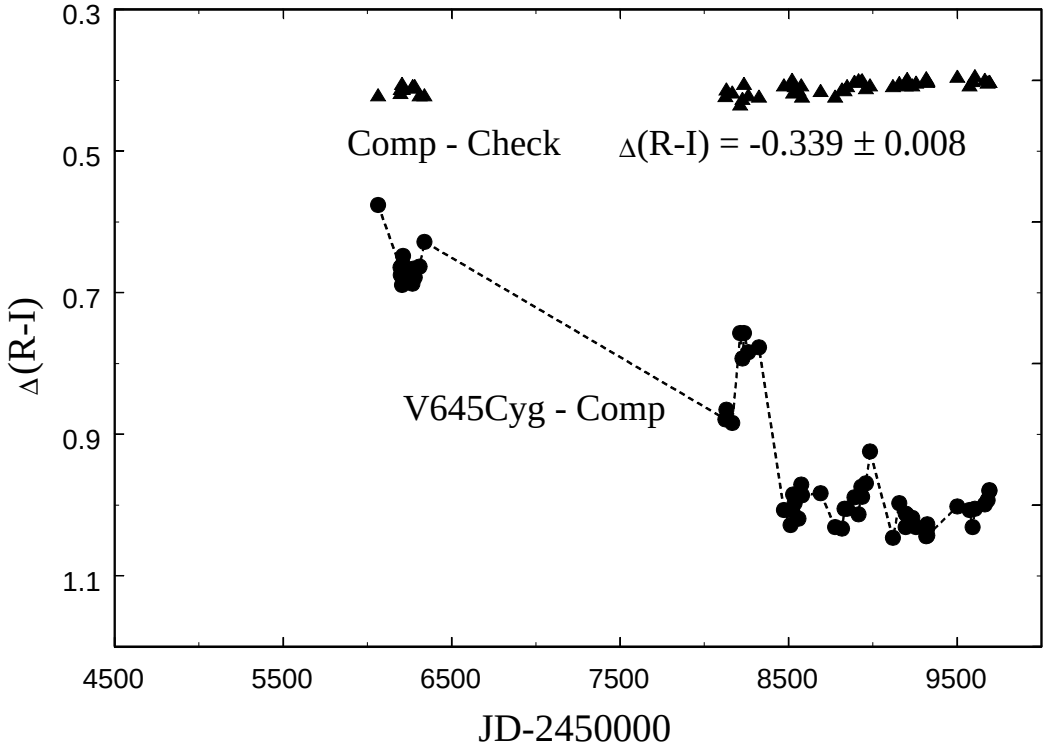

Figure 5. The time dependence of the differences between the $R-I$ color indices of V645 Cyg and the comparison star. Designations are the same as in Fig.1.

with optical brightness variations at time scales of the order of 100 days, is the same in all components of the maser spectrum. Another scenario that can be used to explain the observed variability both in the optical range and in maser lines suggests variations in the accretion rate of matter onto the star, as a result of which the luminosity and temperature of the star change. These changes, in turn, lead to a change of temperature of the dust, radiation of which pumps the CH_3OH masers (Sobolev & Deguchi, 1994). This scenario contradicts the conclusion about the absence of accretion made by Miroshnichenko et al. (2009) based on spectroscopic observations of V645 Cyg. However, it can be that the spectroscopic observations of Miroshnichenko et al. (2009) were carried out at the time of a significant drop in the accretion rate. And finally, the fourth reason for the manifestation of the observed changes in the brightness and color of V645 Cyg in the observed time interval may be further dissipation of the gas-dust cocoon surrounding the star and motion of the star out of cocoon which makes radiation from the star and its heated immediate vicinity more visible. This scenario does not allow one to explain optical brightness variations at time scales of the order of 100 days, which can be quasi-periodic, as well as the corresponding variations in the maser flux density. However, this scenario is applicable to explain the observed monotonic variations in brightness and color of V645 Cyg.

Acknowledgments. A.P.B, A.M.S. and S.Yu.P. were supported by the Foundation for the Advancement of Theoretical Physics and Mathematics "BASIS". S.Yu.G was supported by the Ministry of Science and Higher Education of the Russian Federation under contract 075-15-2020-780.

References:

Asaki, Y., Imai, H., Sobolev, A. M., Parfenov, S. Yu., 2014, *Astrophys.J.*, **787**, article id. 54, 9 pp.

Bowey , J. E., Adamson A. J., & Yates, J. A., 2003, *Mon. Notices Roy. Astron. Soc.*, **340**, 1173

Burns, R. A., Sugiyama, K., Hirota, T., et al.,2020, *Nature Astronomy*, **4**, 506

Clarke, A. J., Lumsden, S. L., Oudmaijer, R. D., et al., 2006,*Astron. & Astrophys.*, **457**, 183

Cohen, M., 1977, *Astrophys. J.*, **215**, 533

Goodrich, R. W., 1986, *Astrophys. J.*, **311**, 882

Kojima, Y., Fujisawa, K., & Motogi, K., 2018, *Astrophysical Masers: Unlocking the Mysteries of the Universe, Proceedings of the International Astronomical Union, IAU Symposium*, **336**, 336

Hamann, F. & Persson, S. E., 1989, *Astrophys. J.*, **339**, 1078.

Hoffmeister, C., Rohlfs, E., & Ahnert, P., 1951, *Veröff. Sternwarte Sonneberg*, **1**, 407

Honma, M., Bushimata, T., Choi, Y. K., et al., 2007, *Publ. Astron. Soc. Japan.*, **59**, 889

Humphreys, R. M., Merrill, K. M., & Black, J. H., 1980, *Astrophys. J.*, **237**, L17

Lada, C. J., Blitz, L., Reid, M. J., & Moran, J. M., 1981, *Astrophys. J.*, **243**, 769

Miroshnichenko, A. S., Hofmann, K.-H., Schertl, D., et al., 2009, *Astron. & Astrophys.*, **498**, 115

Miroshnichenko, A., Ivezić, Ž., Vinković, D., & Elitzur, M., 1999, *Astrophys. J.*, **520**, L115

Morris, M. & Kazes, I., 1982, *Astron. & Astrophys.*, **111**, 239

Parfenov, S. Yu. & Sobolev, A. M., 2014, *Mon. Notices Roy. Astron. Soc.*, **444**, 620

Quiroga-Nuñez, L. H., Immer, K., van Langevelde, H. J., et al., 2019, *Astron. & Astrophys.*, **625**, id. A70, 12pp.

Shenavrin, V. I., Taranova, O. G., & Nadzhip, A. E., 2011, *Astronomy Reports.*, **55**, 31

Shevchenko, V. S., Grankin, K. N., Ibragimov, M. A., et al., 1993, *Astrophys. Space Sci.*, **202**, 121

Sobolev, A. M. & Deguchi, S., 1994, *Astron. & Astrophys.*, **291**, 569

Sobolev, A. M., Gorda, S. Yu., & Davydova, O. A., 2013, *Inform. Bull. Var. Stars*, No. 6061

Szymczak, M., Olech, M., Sarniak, R., et al., 2018, *Mon. Notices Roy. Astron. Soc.*, **474**, 219

Testi, L., Palla, F., & Natta, A. A,, 1998, *Astron. & Astrophys. Suppl. Ser.*, **133**, 81

Torrelles, J. M., Rodriguez, L. F., Canto, J., et al., 1983, *Astrophys. J.*, **274**, 214

Val'tts, I. E., Slysh, V. I., Voronkov, M. A., & Migenes, V., 2002, *Astron. Soc. Pacific Conference Series*, **279**, 279

Zinnecker, H. & Yorke, H. W., 2007, *Ann. Rev. Astron. Astrophys.*, **45**, 481

Table 2: **Night-averaged brightness differences in the V filter of V645 Cyg (ΔV) and check star (ΔC) relative to the comparison star**

Date (DMY)	JD–240000	ΔV	$\pm\sigma$	$\pm\overline{\sigma}$	ΔC	$\pm\sigma$	$\pm\overline{\sigma}$	N
15.04.2009	4937.42857	0.683	0.005	0.001	0.194	0.003	0.001	10
06.05.2009	4958.33519	0.688	0.009	0.003	0.196	0.007	0.002	9
13.05.2009	4965.35769	0.790	0.008	0.002	0.201	0.006	0.001	25
14.05.2009	4966.32331	0.759	0.010	0.002	0.202	0.004	0.001	25
19.05.2009	4971.35191	0.766	0.006	0.001	0.190	0.005	0.001	25
20.05.2009	4972.30408	0.795	0.023	0.008	0.204	0.006	0.002	6
27.05.2009	4979.33769	0.716	0.015	0.003	0.191	0.008	0.002	22
22.07.2009	5035.34787	0.751	0.009	0.002	0.199	0.004	0.001	30
23.07.2009	5036.33920	0.682	0.028	0.006	0.198	0.006	0.002	19
27.07.2009	5040.34753	0.726	0.012	0.002	0.201	0.004	0.001	47
14.09.2009	5089.28315	0.684	0.012	0.002	0.201	0.003	0.001	43
15.09.2009	5090.30562	0.739	0.023	0.007	0.206	0.002	0.001	10
17.09.2009	5092.42973	0.717	0.015	0.003	0.202	0.005	0.001	26
22.10.2009	5127.31837	0.688	0.009	0.001	0.207	0.007	0.001	42
16.11.2009	5152.31745	0.726	0.008	0.002	0.201	0.004	0.001	24
17.11.2009	5153.19977	0.654	0.017	0.003	0.196	0.006	0.001	43
10.12.2009	5176.25266	0.641	0.017	0.002	0.201	0.005	0.001	30
21.01.2010	5218.16453	0.736	0.008	0.001	0.196	0.005	0.001	30
26.01.2010	5223.12589	0.708	0.011	0.002	0.194	0.014	0.001	22
02.02.2010	5230.13721	0.625	0.015	0.003	0.198	0.006	0.001	24
06.03.2010	5262.52940	0.810	0.006	0.002	0.198	0.003	0.001	13
18.03.2010	5274.49065	0.937	0.011	0.004	0.195	0.002	0.001	7
25.03.2010	5281.47928	0.987	0.009	0.002	0.199	0.005	0.001	13
08.04.2010	5295.43740	1.035	0.017	0.004	0.204	0.007	0.002	15
12.05.2010	5329.36131	0.947	0.009	0.002	0.206	0.017	0.004	19
13.05.2010	5330.36267	0.875	0.025	0.006	0.208	0.005	0.001	15
21.07.2010	5399.33910	0.820	0.014	0.002	0.204	0.006	0.001	32
22.07.2010	5400.33782	0.813	0.015	0.002	0.206	0.004	0.001	43
04.08.2010	5413.33688	0.763	0.015	0.002	0.211	0.006	0.001	36
05.08.2010	5414.33714	0.714	0.014	0.002	0.209	0.006	0.001	44
01.09.2010	5441.31360	0.796	0.009	0.002	0.201	0.004	0.001	43
02.09.2010	5442.36225	0.812	0.014	0.002	0.201	0.004	0.001	66
22.09.2010	5462.23904	0.738	0.022	0.004	0.199	0.008	0.002	25
08.10.2010	5478.29459	0.941	0.010	0.001	0.204	0.005	0.001	79
20.10.2010	5490.14572	0.873	0.013	0.003	0.214	0.006	0.002	25
02.12.2010	5533.23815	0.882	0.013	0.002	0.199	0.005	0.001	64
12.12.2010	5543.19488	0.859	0.018	0.002	0.201	0.004	0.001	70
13.12.2010	5544.19371	0.801	0.014	0.002	0.199	0.006	0.001	76
08.01.2011	5570.21433	0.799	0.011	0.002	0.200	0.006	0.001	41
20.01.2011	5582.13821	0.758	0.013	0.002	0.197	0.006	0.001	31
27.04.2011	5679.41057	0.625	0.009	0.002	0.200	0.004	0.001	17
28.04.2011	5680.40164	0.633	0.010	0.002	0.197	0.005	0.001	14
16.05.2012	6064.39120	0.824	0.015	0.004	0.197	0.008	0.002	11
26.09.2012	6197.38419	0.639	0.014	0.004	0.205	0.006	0.002	11
27.09.2012	6198.23936	0.628	0.022	0.005	0.201	0.009	0.003	8

Table 2: **Continued**

Date (DMY)	JD–240000	ΔV	$\pm\sigma$	$\pm\overline{\sigma}$	ΔC	$\pm\sigma$	$\pm\overline{\sigma}$	N
04.10.2012	6205.24359	0.610	0.008	0.004	0.208	0.004	0.001	28
10.10.2012	6211.13611	0.654	0.018	0.005	0.209	0.005	0.001	13
11.10.2012	6212.28667	0.626	0.010	0.001	0.213	0.004	0.001	60
06.12.2012	6268.19165	0.584	0.008	0.002	0.208	0.004	0.001	22
07.12.2012	6269.14436	0.590	0.008	0.002	0.208	0.003	0.001	25
12.12.2012	6274.15618	0.551	0.011	0.002	0.205	0.004	0.001	25
19.12.2012	6281.12896	0.539	0.011	0.002	0.206	0.005	0.001	25
17.01.2013	6310.07494	0.516	0.008	0.003	0.205	0.015	0.007	5
14.02.2013	6338.12007	0.484	0.003	0.001	0.206	0.003	0.001	5
12.08.2013	6517.32602	0.656	0.010	0.001	0.204	0.004	0.001	55
10.10.2013	6576.28931	0.711	0.008	0.001	0.208	0.006	0.001	39
14.07.2014	6853.34689	0.314	0.013	0.002	0.212	0.008	0.001	39
11.09.2014	6912.38557	0.451	0.011	0.001	0.189	0.006	0.001	62
15.09.2015	7281.25513	0.485	0.007	0.001	0.168	0.005	0.001	38
26.04.2017	7870.44585	0.447	0.012	0.004	0.161	0.004	0.001	7
11.10.2017	8038.17950	0.324	0.008	0.002	0.181	0.006	0.001	25
05.01.2018	8124.17500	0.285	0.004	0.001	0.178	0.005	0.001	20
06.01.2018	8125.11670	0.308	0.006	0.001	0.170	0.005	0.001	40
12.01.2018	8131.14580	0.341	0.006	0.001	0.176	0.004	0.001	20
16.02.2018	8166.10420	0.224	0.004	0.001	0.188	0.006	0.002	10
03.04.2018	8212.45700	0.415	0.007	0.001	0.178	0.007	0.002	9
16.04.2018	8225.42570	0.400	0.011	0.003	0.178	0.006	0.001	20
26.04.2018	8235.39240	0.310	0.008	0.002	0.186	0.005	0.001	20
22.05.2018	8261.34380	0.263	0.006	0.001	0.188	0.007	0.002	20
24.07.2018	8324.32700	0.151	0.007	0.002	0.183	0.003	0.001	13
19.12.2018	8472.22850	0.129	0.012	0.003	0.202	0.005	0.001	20
28.01.2019	8512.18820	0.090	0.012	0.003	0.195	0.004	0.001	13
06.02.2019	8521.14650	0.177	0.007	0.002	0.199	0.007	0.002	10
12.02.2019	8527.20200	0.145	0.009	0.003	0.199	0.007	0.002	15
20.02.2019	8535.12500	0.119	0.005	0.002	0.203	0.008	0.004	5
15.03.2019	8558.49310	0.126	0.005	0.002	0.193	0.004	0.001	10
06.04.2019	8580.40970	0.179	0.003	0.001	0.204	0.003	0.001	10
01.04.2019	8575.47010	0.162	0.003	0.001	0.208	0.003	0.001	10
25.07.2019	8690.30330	0.296	0.012	0.003	0.202	0.005	0.001	20
19.10.2019	8776.34880	0.126	0.004	0.001	0.164	0.012	0.004	10
29.11.2019	8817.27748	0.077	0.004	0.001	0.175	0.017	0.003	30
14.12.2019	8832.20632	0.030	0.014	0.004	0.175	0.004	0.001	15
29.12.2019	8847.18480	–0.078	0.004	0.001	0.195	0.003	0.001	15
12.02.2020	8891.15382	–0.067	0.005	0.002	0.186	0.007	0.003	5
05.03.2020	8914.54355	–0.117	0.004	0.001	0.159	0.006	0.002	11
23.03.2020	8932.47483	–0.064	0.006	0.002	0.155	0.005	0.001	15
27.03.2020	8936.44622	–0.054	0.005	0.001	0.168	0.004	0.001	18
19.04.2020	8959.38451	–0.003	0.015	0.002	0.172	0.010	0.003	10

Table 2: **Continued**

Date (DMY)	JD–240000	ΔV	$\pm\sigma$	$\pm\overline{\sigma}$	ΔC	$\pm\sigma$	$\pm\overline{\sigma}$	N
13.05.2020	8983.35573	0.019	0.005	0.001	0.167	0.005	0.001	20
26.09.2020	9119.30094	–0.070	0.007	0.001	0.163	0.003	0.001	29
02.10.2020	9125.37666	–0.125	0.013	0.003	0.161	0.010	0.002	20
28.10.2020	9151.33432	–0.193	0.009	0.002	0.152	0.008	0.002	23
03.11.2020	9157.40251	–0.205	0.006	0.001	0.158	0.006	0.002	16
10.12.2020	9194.22652	–0.211	0.005	0.001	0.159	0.003	0.001	25
11.12.2020	9195.22465	–0.200	0.004	0.001	0.157	0.004	0.001	23
19.12.2020	9203.16506	–0.215	0.004	0.001	0.156	0.005	0.001	20
18.01.2021	9233.18459	–0.230	0.005	0.001	0.158	0.006	0.001	12
10.02.2021	9256.12148	–0.143	0.007	0.001	0.135	0.005	0.001	15
12.04.2021	9317.43391	–0.112	0.005	0.001	0.174	0.003	0.001	25
16.04.2021	9321.43617	–0.125	0.003	0.001	0.165	0.003	0.001	17
17.04.2021	9322.38562	–0.072	0.005	0.001	0.171	0.004	0.001	39
18.04.2021	9323.40756	–0.078	0.004	0.001	0.173	0.003	0.001	34
13.10.2021	9501.26582	–0.223	0.003	0.001	0.166	0.003	0.001	18
14.10.2021	9502.35009	–0.252	0.004	0.001	0.159	0.005	0.001	30
25.12.2021	9574.17410	–0.204	0.008	0.001	0.153	0.004	0.001	41
12.01.2022	9592.12339	–0.237	0.006	0.001	0.161	0.007	0.001	20
26.01.2022	9606.13106	–0.257	0.008	0.002	0.168	0.009	0.002	20
25.03.2022	9664.45067	–0.185	0.004	0.001	0.174	0.004	0.001	35
11.04.2022	9681.40484	–0.270	0.005	0.001	0.163	0.006	0.001	20
21.04.2022	9691.39852	–0.166	0.004	0.001	0.176	0.004	0.001	33
22.04.2022	9692.39289	–0.195	0.006	0.001	–0.169	0.003	0.001	30

Table 3: **Night-averaged brightness differences in the R filter of V645 Cyg (ΔR) and check star (ΔC) relative to the comparison star**

Date (DMY)	JD–240000	ΔR	$\pm\sigma$	$\pm\overline{\sigma}$	ΔC	$\pm\sigma$	$\pm\overline{\sigma}$	N
15.04.2009	4937.43140	0.198	0.004	0.001	0.510	0.004	0.002	10
17.11.2009	5153.21515	0.212	0.013	0.002	0.501	0.010	0.001	46
21.01.2010	5218.16560	0.271	0.008	0.002	0.499	0.004	0.001	29
26.01.2010	5223.13941	0.260	0.012	0.002	0.500	0.004	0.001	28
02.02.2010	5230.14237	0.199	0.017	0.004	0.506	0.005	0.001	18
06.03.2010	5262.53163	0.353	0.006	0.002	0.507	0.005	0.001	13
18.03.2010	5274.50131	0.448	0.005	0.001	0.508	0.005	0.001	10
25.03.2010	5281.48204	0.467	0.006	0.002	0.513	0.003	0.001	12
08.04.2010	5295.44222	0.484	0.009	0.002	0.518	0.012	0.003	18
12.05.2010	5329.37148	0.463	0.007	0.002	0.516	0.010	0.003	12
13.05.2010	5330.36559	0.408	0.016	0.004	0.517	0.008	0.002	12
21.07.2010	5399.34054	0.364	0.007	0.001	0.515	0.004	0.001	32
22.07.2010	5400.33931	0.358	0.008	0.001	0.513	0.005	0.001	43
04.08.2010	5413.33720	0.313	0.009	0.001	0.525	0.005	0.001	40
05.08.2010	5414.33911	0.271	0.010	0.002	0.524	0.008	0.001	44
01.09.2010	5441.34618	0.341	0.015	0.002	0.507	0.008	0.001	41
02.09.2010	5442.36419	0.349	0.006	0.001	0.515	0.004	0.001	66
22.09.2010	5462.24106	0.317	0.014	0.003	0.505	0.010	0.002	22
08.10.2010	5478.29670	0.449	0.009	0.001	0.513	0.004	0.001	78
20.10.2010	5490.15031	0.403	0.009	0.002	0.507	0.006	0.001	26
02.12.2010	5533.24075	0.425	0.013	0.002	0.500	0.007	0.001	65
12.12.2010	5543.20149	0.398	0.017	0.002	0.506	0.006	0.001	68
13.12.2010	5544.19296	0.351	0.013	0.002	0.503	0.007	0.001	73
08.01.2011	5570.21428	0.343	0.011	0.002	0.505	0.007	0.001	40
20.01.2011	5582.14021	0.320	0.013	0.002	0.503	0.007	0.001	32
27.04.2011	5679.41259	0.208	0.005	0.001	0.509	0.005	0.001	17
28.04.2011	5680.40578	0.216	0.005	0.001	0.506	0.005	0.002	16
16.05.2012	6064.39120	0.248	0.014	0.004	0.504	0.008	0.002	12
26.09.2012	6197.38655	0.120	0.016	0.006	0.516	0.008	0.002	11
27.09.2012	6198.23906	0.127	0.015	0.005	0.511	0.007	0.002	8
04.10.2012	6205.24509	0.104	0.005	0.001	0.520	0.003	0.001	27
10.10.2012	6211.13493	0.160	0.011	0.003	0.525	0.005	0.001	13
11.10.2012	6212.28589	0.139	0.008	0.001	0.522	0.005	0.001	61
06.12.2012	6268.19709	0.080	0.007	0.001	0.518	0.006	0.001	23
07.12.2012	6269.14649	0.097	0.009	0.002	0.516	0.003	0.001	25
12.12.2012	6274.15831	0.055	0.006	0.001	0.515	0.005	0.001	25
19.12.2012	6281.12896	0.043	0.010	0.002	0.513	0.006	0.001	25
17.01.2013	6310.07528	0.028	0.021	0.010	0.504	0.015	0.006	6
14.02.2013	6338.11821	–0.001	0.007	0.003	0.527	0.004	0.001	6
12.08.2013	6517.32602	0.109	0.006	0.001	0.514	0.006	0.001	55
10.10.2013	6576.28931	0.198	0.005	0.001	0.519	0.009	0.001	39
14.07.2014	6853.34795	–0.293	0.011	0.002	0.517	0.006	0.001	45
11.09.2014	6912.38674	–0.227	0.005	0.001	0.493	0.006	0.001	70
15.09.2015	7281.26488	–0.178	0.005	0.001	0.472	0.007	0.001	42
26.04.2017	7870.44698	–0.305	0.005	0.002	0.464	0.006	0.002	8
11.10.2017	8038.17950	–0.378	0.008	0.002	0.500	0.009	0.002	24
05.01.2018	8124.17500	–0.376	0.005	0.001	0.496	0.003	0.001	20

Table 3: **Continued**

Date (DMS)	JD–240000	ΔR	$\pm\sigma$	$\pm\overline{\sigma}$	ΔC	$\pm\sigma$	$\pm\overline{\sigma}$	N
06.01.2018	8125.11670	–0.332	0.006	0.001	0.490	0.005	0.001	40
12.01.2018	8131.14580	–0.313	0.006	0.001	0.481	0.005	0.001	20
16.02.2018	8166.10420	–0.401	0.007	0.001	0.499	0.006	0.002	10
03.04.2018	8212.45700	–0.175	0.005	0.001	0.487	0.004	0.001	10
16.04.2018	8225.42570	–0.205	0.009	0.003	0.491	0.006	0.001	20
26.04.2018	8235.39240	–0.287	0.007	0.002	0.490	0.006	0.001	20
22.05.2018	8261.34380	–0.350	0.010	0.001	0.502	0.007	0.002	19
24.07.2018	8324.32700	–0.477	0.006	0.002	0.499	0.005	0.001	13
19.12.2018	8472.22850	–0.533	0.007	0.003	0.505	0.008	0.002	20
28.01.2019	8512.18820	–0.603	0.010	0.003	0.497	0.006	0.001	16
06.02.2019	8521.14650	–0.504	0.007	0.002	0.494	0.006	0.002	10
12.02.2019	8527.20200	–0.524	0.007	0.003	0.502	0.005	0.001	15
20.02.2019	8535.12500	–0.546	0.003	0.002	0.507	0.003	0.001	5
15.03.2019	8558.49310	–0.548	0.004	0.002	0.495	0.004	0.001	10
06.04.2019	8580.40970	–0.518	0.007	0.001	0.501	0.007	0.002	10
01.04.2019	8575.47010	–0.501	0.004	0.001	0.504	0.004	0.001	10
25.07.2019	8690.30330	–0.379	0.004	0.003	0.499	0.004	0.001	18
19.10.2019	8776.34880	–0.546	0.005	0.001	0.465	0.005	0.002	10
29.11.2019	8817.27748	–0.628	0.006	0.001	0.477	0.006	0.001	30
14.12.2019	8832.20632	–0.653	0.009	0.002	0.473	0.004	0.001	15
29.12.2019	8847.18596	–0.784	0.007	0.002	0.498	0.004	0.001	15
12.02.2020	8891.15380	–0.774	0.007	0.003	0.473	0.007	0.003	5
05.03.2020	8914.54356	–0.835	0.003	0.001	0.473	0.004	0.001	10
23.03.2020	8932.47486	–0.768	0.007	0.002	0.482	0.007	0.002	15
27.03.2020	8936.44622	–0.765	0.005	0.001	0.497	0.005	0.001	18
19.04.2020	8959.38451	–0.729	0.011	0.004	0.489	0.006	0.002	10
13.05.2020	8983.35573	–0.676	0.005	0.001	0.493	0.007	0.001	20
26.09.2020	9119.30094	–0.817	0.011	0.002	0.488	0.007	0.001	31
02.10.2020	9125.38042	–0.850	0.015	0.004	0.492	0.015	0.003	20
28.10.2020	9151.33478	–0.918	0.011	0.002	0.479	0.010	0.002	23
03.11.2020	9157.40251	–0.940	0.009	0.002	0.488	0.012	0.003	16
10.12.2020	9194.22652	–0.927	0.007	0.001	0.478	0.004	0.001	25
11.12.2020	9195.22465	–0.892	0.007	0.001	0.485	0.004	0.001	23
19.12.2020	9203.16506	–0.913	0.004	0.001	0.477	0.005	0.001	20
18.01.2021	9233.18459	–0.956	0.004	0.001	0.483	0.009	0.002	12
10.02.2021	9256.12148	–0.900	0.006	0.001	0.456	0.007	0.001	15
12.04.2021	9317.43391	–0.886	0.004	0.001	0.494	0.003	0.001	25
16.04.2021	9321.43617	–0.890	0.004	0.001	0.486	0.005	0.001	17
17.04.2021	9322.38562	–0.821	0.005	0.001	0.490	0.005	0.001	39
18.04.2021	9323.40756	–0.849	0.005	0.001	0.493	0.003	0.001	35
13.10.2021	9501.27132	–0.964	0.004	0.001	0.488	0.005	0.001	18
14.10.2021	9502.31430	–0.997	0.011	0.002	0.477	0.006	0.001	30
25.12.2021	9574.17410	–0.934	0.006	0.001	0.471	0.009	0.001	41
12.01.2022	9592.12339	–0.972	0.006	0.001	0.479	0.005	0.001	20
26.01.2022	9606.13106	–0.971	0.016	0.004	0.494	0.010	0.002	20
25.03.2022	9664.45067	–0.918	0.005	0.001	0.493	0.006	0.001	35
11.04.2022	9681.40484	–1.016	0.006	0.001	0.487	0.005	0.001	20
21.04.2022	9691.39852	–0.903	0.005	0.001	0.501	0.005	0.001	33
22.04.2022	9692.39289	–0.929	0.005	0.001	0.491	0.004	0.001	30

Table 4: **Night-averaged brightness differences in the I filter of V645 Cyg (ΔI) and check star (ΔC) relative to the comparison star**

Date (DMY)	JD–240000	ΔR	$\pm\sigma$	$\pm\overline{\sigma}$	ΔC	$\pm\sigma$	$\pm\overline{\sigma}$	N
16.05.2012	6064.39120	–0.328	0.006	0.002	0.832	0.009	0.003	12
26.09.2012	6197.38655	–0.544	0.014	0.005	0.847	0.006	0.002	8
27.09.2012	6198.23906	–0.548	0.014	0.005	0.848	0.014	0.005	9
04.10.2012	6205.24509	–0.585	0.007	0.001	0.864	0.005	0.001	25
10.10.2012	6211.13493	–0.500	0.008	0.002	0.862	0.007	0.002	11
11.10.2012	6212.28589	–0.509	0.008	0.001	0.861	0.006	0.001	61
06.12.2012	6268.19709	–0.607	0.006	0.001	0.857	0.006	0.001	23
07.12.2012	6269.14649	–0.573	0.005	0.001	0.857	0.005	0.001	25
12.12.2012	6274.15831	–0.611	0.006	0.001	0.854	0.005	0.001	24
19.12.2012	6281.12896	–0.635	0.007	0.001	0.854	0.007	0.001	25
17.01.2013	6310.07528	–0.635	0.009	0.004	0.832	0.007	0.003	5
14.02.2013	6338.11821	–0.629	0.004	0.002	0.855	0.005	0.002	6
06.01.2018	8125.11670	–1.211	0.008	0.001	0.837	0.005	0.001	40
12.01.2018	8131.14580	–1.178	0.006	0.001	0.837	0.008	0.002	20
16.02.2018	8166.10420	–1.285	0.005	0.002	0.851	0.007	0.002	10
03.04.2018	8212.45700	–0.932	0.007	0.002	0.822	0.004	0.001	9
16.04.2018	8225.42570	–0.998	0.006	0.001	0.834	0.006	0.001	20
26.04.2018	8235.39240	–1.044	0.006	0.001	0.854	0.006	0.001	20
22.05.2018	8261.34380	–1.134	0.010	0.002	0.850	0.008	0.002	19
24.07.2018	8324.32700	–1.254	0.004	0.001	0.845	0.003	0.001	13
19.12.2018	8472.22850	–1.540	0.006	0.001	0.847	0.009	0.002	20
28.01.2019	8512.18820	–1.631	0.014	0.003	0.840	0.009	0.002	16
06.02.2019	8521.14650	–1.511	0.010	0.003	0.844	0.007	0.002	10
12.02.2019	8527.20200	–1.509	0.008	0.002	0.834	0.008	0.002	15
20.02.2019	8535.12500	–1.543	0.008	0.003	0.848	0.005	0.002	5
15.03.2019	8558.49310	–1.567	0.007	0.002	0.830	0.005	0.002	10
01.04.2019	8575.47010	–1.472	0.005	0.002	0.843	0.004	0.001	10
06.04.2019	8580.40970	–1.504	0.007	0.002	0.830	0.008	0.003	10
25.07.2019	8690.30330	–1.362	0.008	0.002	0.833	0.004	0.001	16
19.10.2019	8776.34880	–1.577	0.008	0.002	0.791	0.002	0.001	10
29.11.2019	8817.27750	–1.661	0.007	0.001	0.813	0.007	0.001	30
14.12.2019	8832.20630	–1.658	0.006	0.001	0.808	0.005	0.001	15
29.12.2019	8847.18683	–1.789	0.010	0.003	0.839	0.007	0.002	15
12.02.2020	8891.15580	–1.763	0.006	0.003	0.820	0.009	0.004	5
05.03.2020	8914.54357	–1.848	0.015	0.004	0.822	0.006	0.002	9
23.03.2020	8932.47486	–1.742	0.009	0.002	0.830	0.006	0.002	15
27.03.2020	8936.44622	–1.753	0.017	0.003	0.846	0.006	0.001	18
19.04.2020	8959.38451	–1.699	0.010	0.004	0.828	0.013	0.004	10
13.05.2020	8983.35573	–1.601	0.015	0.002	0.836	0.006	0.001	20
26.09.2020	9119.29258	–1.864	0.017	0.003	0.830	0.013	0.002	31
03.11.2020	9157.40251	–1.937	0.012	0.003	0.834	0.009	0.002	16
10.12.2020	9194.22652	–1.948	0.006	0.001	0.825	0.006	0.001	25
11.12.2020	9195.22465	–1.904	0.009	0.002	0.827	0.010	0.002	23
19.12.2020	9203.16506	–1.927	0.008	0.002	0.828	0.009	0.002	20

Table 4: **Continued**

Date (DMY)	JD–240000	ΔI	$\pm\sigma$	$\pm\overline{\sigma}$	ΔC	$\pm\sigma$	$\pm\overline{\sigma}$	N
18.01.2021	9233.18459	–1.974	0.012	0.004	0.825	0.013	0.004	10
10.02.2021	9256.12148	–1.931	0.011	0.002	0.802	0.014	0.003	15
12.04.2021	9317.43391	–1.926	0.007	0.001	0.845	0.005	0.001	25
16.04.2021	9321.43617	–1.924	0.006	0.001	0.833	0.007	0.001	17
17.04.2021	9322.38562	–1.848	0.008	0.001	0.838	0.008	0.001	39
18.04.2021	9323.40756	–1.892	0.007	0.001	0.842	0.005	0.001	34
13.10.2021	9501.26722	–1.966	0.008	0.001	0.842	0.010	0.002	18
25.12.2021	9574.17410	–1.941	0.008	0.001	0.813	0.013	0.002	41
12.01.2022	9592.12339	–2.003	0.009	0.002	0.827	0.008	0.002	20
26.01.2022	9606.13106	–1.976	0.012	0.003	0.849	0.014	0.003	20
25.03.2022	9664.45067	–1.917	0.006	0.001	0.847	0.006	0.001	35
11.04.2022	9681.40484	–2.009	0.007	0.002	0.833	0.008	0.002	20
21.04.2022	9691.39852	–1.883	0.007	0.002	0.848	0.007	0.001	33
22.04.2022	9692.39289	–1.908	0.006	0.001	0.838	0.006	0.001	30

Table 5: **The night-averaged differences between the color indices of V645 Cyg, $\Delta(V-R)$, and the check star, $\Delta(V-R)_C$, relative to the comparison star**

Date (DMY)	JD–240000	$\Delta(V-R)$	$\Delta(V-R)_C$	N
15.04.2009	4937.43140	0.485	–0.316	10
17.11.2009	5153.21515	0.442	–0.305	46
21.01.2010	5218.16560	0.465	–0.303	29
26.01.2010	5223.13941	0.448	–0.306	28
02.02.2010	5230.14237	0.426	–0.308	18
06.03.2010	5262.53163	0.457	–0.309	13
18.03.2010	5274.50131	0.489	–0.313	10
25.03.2010	5281.48204	0.520	–0.314	12
08.04.2010	5295.44222	0.551	–0.314	18
12.05.2010	5329.37148	0.484	–0.310	12
13.05.2010	5330.36559	0.467	–0.309	12
21.07.2010	5399.34054	0.456	–0.311	32
22.07.2010	5400.33931	0.455	–0.307	43
04.08.2010	5413.33720	0.450	–0.314	40
05.08.2010	5414.33911	0.443	–0.315	44
01.09.2010	5441.34618	0.455	–0.306	41
02.09.2010	5442.36419	0.463	–0.314	66
22.09.2010	5462.24106	0.421	–0.306	22
08.10.2010	5478.29670	0.492	–0.309	78
20.10.2010	5490.15031	0.470	–0.293	26
02.12.2010	5533.24075	0.457	–0.301	65
12.12.2010	5543.20149	0.461	–0.305	68
13.12.2010	5544.19296	0.450	–0.304	73
08.01.2011	5570.21428	0.456	–0.305	40
20.01.2011	5582.14021	0.438	–0.306	32
27.04.2011	5679.41259	0.417	–0.309	17
28.04.2011	5680.40578	0.417	–0.309	16
16.05.2012	6064.39120	0.576	–0.307	12
26.09.2012	6197.38655	0.519	–0.311	11
27.09.2012	6198.23906	0.501	–0.310	8
04.10.2012	6205.24509	0.506	–0.312	27
10.10.2012	6211.13493	0.494	–0.316	13
11.10.2012	6212.28589	0.487	–0.309	61
06.12.2012	6268.19709	0.504	–0.310	23
07.12.2012	6269.14649	0.493	–0.308	25
12.12.2012	6274.15831	0.496	–0.310	25
19.12.2012	6281.12896	0.496	–0.307	25
17.01.2013	6310.07528	0.488	–0.299	6
14.02.2013	6338.11821	0.485	–0.321	6
12.08.2013	6517.32602	0.547	–0.310	55
10.10.2013	6576.28931	0.513	–0.311	39
14.07.2014	6853.34795	0.607	–0.305	45
11.09.2014	6912.38674	0.678	–0.304	70
15.09.2015	7281.26488	0.663	–0.304	42
26.04.2017	7870.44698	0.752	–0.303	8
11.10.2017	8038.17950	0.702	–0.319	24
05.01.2018	8124.17500	0.661	–0.318	20

Table 5: **Continued**

Date (DMY)	JD–240000	$\Delta(V-R)$	$\Delta(V-R)_C$	N
06.01.2018	8125.11670	0.640	–0.320	40
12.01.2018	8131.14580	0.654	–0.305	20
16.02.2018	8166.10420	0.625	–0.311	10
03.04.2018	8212.45700	0.590	–0.309	10
16.04.2018	8225.42570	0.605	–0.313	20
26.04.2018	8235.39240	0.597	–0.304	20
22.05.2018	8261.34380	0.613	–0.314	19
24.07.2018	8324.32700	0.628	–0.316	13
19.12.2018	8472.22850	0.662	–0.303	20
28.01.2019	8512.18820	0.693	–0.302	16
06.02.2019	8521.14650	0.681	–0.295	10
12.02.2019	8527.20200	0.669	–0.303	15
20.02.2019	8535.12500	0.665	–0.304	5
15.03.2019	8558.49310	0.674	–0.302	10
06.04.2019	8580.40970	0.697	–0.297	10
01.04.2019	8575.47010	0.663	–0.296	10
25.07.2019	8690.30330	0.675	–0.297	18
19.10.2019	8776.34880	0.672	–0.301	10
29.11.2019	8817.27748	0.705	–0.302	30
14.12.2019	8832.20632	0.683	–0.298	15
29.12.2019	8847.18596	0.706	–0.303	15
12.02.2020	8891.15380	0.707	–0.307	5
05.03.2020	8914.54356	0.718	–0.314	10
23.03.2020	8932.47486	0.704	–0.327	15
27.03.2020	8936.44622	0.711	–0.329	18
19.04.2020	8959.38451	0.726	–0.319	10
13.05.2020	8983.35573	0.695	–0.327	20
26.09.2020	9119.30094	0.747	–0.326	31
02.10.2020	9125.38042	0.725	–0.331	20
28.10.2020	9151.33478	0.725	–0.327	23
03.11.2020	9157.40251	0.735	–0.330	16
10.12.2020	9194.22652	0.716	–0.319	25
11.12.2020	9195.22465	0.692	–0.328	23
19.12.2020	9203.16506	0.698	–0.321	20
18.01.2021	9233.18459	0.726	–0.325	12
10.02.2021	9256.12148	0.757	–0.321	15
12.04.2021	9317.43391	0.774	–0.320	25
16.04.2021	9321.43617	0.765	–0.321	17
17.04.2021	9322.38562	0.749	–0.319	39
18.04.2021	9323.40756	0.771	–0.320	35
13.10.2021	9501.27132	0.741	–0.322	18
14.10.2021	9502.31430	0.745	–0.318	30
25.12.2021	9574.17410	0.730	–0.318	41
12.01.2022	9592.12339	0.735	–0.318	20
26.01.2022	9606.13106	0.714	–0.326	20
25.03.2022	9664.45067	0.733	–0.319	35
11.04.2022	9681.40484	0.746	–0.324	20
21.04.2022	9691.39852	0.737	–0.332	33
22.04.2022	9692.39289	0.734	–0.322	30

Table 6: **The night-averaged differences between the color indices of V645 Cyg, $\Delta(R-I)$, and the check star, $\Delta(R-I)_C$, relative to the comparison star**

Date (DMY)	JD–240000	$\Delta(R-I)$	$\Delta(R-I)_C$	N
16.05.2012	6064.39120	0.576	–0.328	12
26.09.2012	6197.38655	0.664	–0.331	8
27.09.2012	6198.23906	0.675	–0.337	9
04.10.2012	6205.24509	0.689	–0.344	25
10.10.20012	6211.13493	0.660	–0.337	11
11.10.2012	6212.28589	0.648	–0.339	61
06.12.2012	6268.19709	0.687	–0.339	23
07.12.2012	6269.14649	0.670	–0.341	25
12.12.2012	6274.15831	0.666	–0.339	24
19.12.2012	6281.12896	0.678	–0.341	25
17.01.2013	6310.07528	0.663	–0.328	5
14.02.2013	6338.11821	0.628	–0.328	6
06.01.2018	8125.11670	0.879	–0.327	40
12.01.2018	8131.14580	0.865	–0.336	20
16.02.2018	8166.10420	0.884	–0.332	10
03.04.2018	8212.45700	0.757	–0.315	9
16.04.2018	8225.42570	0.793	–0.323	20
26.04.2018	8235.39240	0.757	–0.344	20
22.05.2018	8261.34380	0.784	–0.328	19
24.07.2018	8324.32700	0.777	–0.326	13
19.12.2018	8472.22850	1.007	–0.342	20
28.01.2019	8512.18820	1.028	–0.343	16
06.02.2019	8521.14650	1.007	–0.350	10
12.02.2019	8527.20200	0.985	–0.332	15
20.02.2019	8535.12500	0.997	–0.341	5
15.03.2019	8558.49310	1.019	–0.335	10
01.04.2019	8575.47010	0.971	–0.342	10
06.04.2019	8580.40970	0.986	–0.326	10
25.07.2019	8690.30330	0.983	–0.334	16
19.10.2019	8776.34880	1.031	–0.326	10
29.11.2019	8817.27750	1.033	–0.336	30
14.12.2019	8832.20630	1.005	–0.335	15
29.12.2019	8847.18683	1.005	–0.341	15
12.02.2020	8891.15580	0.989	–0.347	5
05.03.2020	8914.54357	1.013	–0.349	9
23.03.2020	8932.47486	0.974	–0.348	15
27.03.2020	8936.44622	0.988	–0.349	18
19.04.2020	8959.38451	0.969	–0.338	10
13.05.2020	8983.35573	0.924	–0.342	20
26.09.2020	9119.29258	1.046	–0.341	31
03.11.2020	9157.40251	0.997	–0.345	16
10.12.2020	9194.22652	1.031	–0.347	25
11.12.2020	9195.22465	1.012	–0.342	23
19.12.2020	9203.16506	1.014	–0.351	20

Table 6: **Continued**

Date (DMY)	JD–240000	$\Delta(R-I)$	$\Delta(R-I)_C$	N
18.01.2021	9233.18459	1.018	–0.342	10
10.02.2021	9256.12148	1.031	–0.346	15
12.04.2021	9317.43391	1.044	–0.352	25
16.04.2021	9321.43617	1.034	–0.347	17
17.04.2021	9322.38562	1.027	–0.348	39
18.04.2021	9323.40756	1.043	–0.349	34
13.10.2021	9501.26722	1.002	–0.354	18
25.12.2021	9574.17410	1.007	–0.342	41
12.01.2022	9592.12339	1.031	–0.348	20
26.01.2022	9606.13106	1.005	–0.355	20
25.03.2022	9664.45067	0.999	–0.350	35
11.04.2022	9681.40484	0.993	–0.346	20
21.04.2022	9691.39852	0.980	–0.347	33
22.04.2022	9692.39289	0.979	–0.347	30